* Manuscript
Click here to view linked References

Exploring typhoon variability over the mid-to-late Holocene: evidence of extreme coastal flooding from Kamikoshiki, Japan

Jonathan D. Woodruff[1*], Jeffrey P. Donnelly[2], and Akiko Okusu[3]

Submitted to *Quaternary Science Reviews*

[1]Department of Geosciences, University of Massachusetts, Amherst, MA
[2]Department of Geology and Geophysics, Woods Hole Oceanographic Institution, Woods Hole, MA
[3]Department of Biology, Simmons College, Boston, MA

Abstract

Sediment cores from two coastal lakes located on the island of Kamikoshiki in southwestern Japan (Lake Namakoike and Lake Kaiike) provide evidence for the response of a backbarrier beach system to episodic coastal inundation over the last 6400 years. Subbottom seismic surveys exhibit acoustically laminated, parallel to subparallel seismic reflectors, intermittently truncated by erosional unconformities. Sediment cores collected from targeted depocenters in both lakes contain finely laminated organic mud interbedded with coarse grained units, with depths of coarse deposits concurrent with prominent seismic reflectors. The timing of the youngest deposit at Kamikoshiki correlates to the most recently documented breach in the barrier during a typhoon in 1951 AD. Assuming this modern deposit provides an analog for identifying past events, paleo-typhoons may be reconstructed from layers exhibiting an increase in grain-size, a break in fine-scale stratigraphy, and elevated Sr concentrations.

Periods of barrier breaching are concurrent with an increase in El Niño frequency, indicating that the El Niño/Southern Oscillation has potentially played a key role in governing typhoon variability during the mid-to-late Holocene. An inverse correlation is observed between tropical cyclone reconstructions from the western North Atlantic and the Kamikoshiki site, which may indicate an oscillating pattern in tropical cyclone activity between the western Northern Atlantic and the western North Pacific, or at least between the western Northern Atlantic and regions encompassing southern Japan. The two *kamikaze* typhoons which contributed to the failed Mongol invasions of Japan in

1274 AD and 1281 AD occur during a period with more frequent marine-sourced deposition at the site, suggesting the events took place during a period of greater regional typhoon activity.

1. Introduction

Approximately a third of all tropical cyclones in the world form within the western North Pacific (Gray, 1968; Henderson-Sellers et al., 1998), making it the most active tropical cyclone basin on earth. However, relatively little is known about how shifts in climate alter the frequency, intensity, and tracks of typhoons in this region (here "typhoon" is used to describe tropical cyclones forming in the northwest Pacific, while "hurricane" describes tropical cyclones forming in the western North Atlantic and eastern North Pacific). Large uncertainties exist in part because reliable instrumental records for typhoons only extend back to 1945 AD (Chu et al., 2002), prohibiting the analysis of typhoon variability on timescales longer than a few decades. Significantly longer data sets for typhoon occurrences are therefore required to elucidate the dominant climatic controls of typhoon activity on the centennial-to-millennial timescales.

Natural archives of tropical cyclones can extend the documented record well beyond the observational record and help identify how tropical cyclone activity has responded to past shifts in climate (Frappier et al., 2007a; Nott, 2004). Geologic proxies for tropical cyclones include negative $\delta^{18}O$ anomalies in speleothems and tree rings (Frappier et al., 2007b; Malmquist, 1997; Miller et al., 2006; Nott et al., 2007), storminduced beach ridges and scarps (Buynevich et al., 2007; Nott and Hayne, 2001), cyclone-transported boulder deposits (Scheffers and Scheffers, 2006; Spiske et al., 2008; Suzuki et al., 2008; Yu et al., 2004), preserved offshore beds and bedforms (Duke, 1985; Ito et al., 2001; Keen et al., 2004; Keen et al., 2006), and sedimentary archives of freshwater flooding events (Besonen et al., 2008; Grossman, 2001). In addition, overwash deposits preserved within backbarrier beach environments can be a particularly effective proxy of long-term tropical cyclone variability (Donnelly, 2005; Donnelly et al., 2001a; Donnelly et al., 2004; Donnelly et al., 2001b; Donnelly and Webb, 2004; Donnelly and Woodruff, 2007; Emery, 1969; Liu and Fearn, 1993; Liu and Fearn, 2000; Scileppi and Donnelly, 2007; Woodruff et al., 2008b), during intervals when coastal morphology has remained fairly stable (Donnelly and Giosan, 2008; Lambert et al., 2003; Otvos, 1999; Otvos, 2002).

Recent compilations of millennial-scale hurricane reconstructions from the western North Atlantic indicate basin wide fluctuations in activity over the last 5000 years (Donnelly and Woodruff, 2007; Scileppi and Donnelly, 2007; Woodruff et al., 2008a). Although these reconstructions are still limited in number, stochastic simulations indicate that observed trends are statistically significant and unlikely to occur under the present climate (Woodruff et al., 2008a). Comparisons with previously developed climate proxies indicate that past increases in hurricane activity in the western North Atlantic occur during periods of less frequent El Niño events and stronger West African monsoons, suggesting that these climatic phenomena have played a significant role in modulating hurricane activity in the western North Atlantic over the mid-to-late Holocene (Donnelly and Woodruff, 2007).

The El Niño/Southern Oscillation (ENSO) strongly affects tropical cyclone activity in both the western North Atlantic and the western North Pacific; however, its influence is different within the two basins. In the western North Atlantic, vertical wind shear is generally greater during El Niño years, which inhibits the formation of tropical cyclones (Bove et al., 1998; Goldenberg and Shapiro, 1996; Gray, 1984). In the western North Pacific, the overall number of tropical cyclones is less affected by ENSO (Wang and Chan, 2002); however, the mean genesis location for typhoons generally shifts to the southeast during El Niño years (Chan, 1985; Lander, 1994). This shift results in longer lasting typhoons (Wang and Chan, 2002), which generally become more intense (Camargo and Sobel, 2005; Chan, 2007). In addition, typhoons during El Niño years tend to recurve to the northeast (Wang and Chan, 2002), which may increase the likelihood of typhoon making landfall in Japan and South Korea (Elsner and Liu, 2003).

In comparison to the western North Atlantic, centennial-to-millennial scale typhoon reconstructions from the western North Pacific are far more limited. Historical government documents of typhoon landfalls from the Guangdong Providence in Southern China extend back 1000 years, although complete records for typhoon strikes to the region are likely only reliable back to 1600 AD (Chan and Shi, 2000; Lee and Hsu, 1989; Liu et al., 2001; Qiao and Tang, 1993). Arakawa et al. (1961) has also put together an assemblage of historical documents describing typhoon occurrences in Japan between 701 AD and 1865 AD. Recent efforts are also underway to compile additional Japanese records for typhoon landfalls (e.g. Grossman and Zaiki, 2007). Paleo-typhoon reconstructions have also been constructed from boulder and atoll deposits (Yu et al., 2004; Zhu et al., 1991), but to date no millennial-scale typhoon records exist in regions other than the South China Sea.

Long-term reconstructions of typhoon variability from southern Japan may help to identify the dominant processes controlling typhoon activity in the western North Pacific on timescales greater than annual-to-decadal. Towards this end we examine the mid-to-late Holocene development of two backbarrier lagoons on the island of Kamikoshiki, Japan, and assess the depositional response of each lake to typhoon-induced breaches in the coastal barrier.

2. Study area

The small island of Kamikoshiki (~60 km^2) is situated approximately 30 km to the west of the southern Kyushu, and is the northern most island of the Koshiki-jima archipelago (Fig. 1). Locally nicknamed "Typhoon Ginza" after one of Tokyo's most popular shopping district, the island is frequently struck by typhoons. According to the "best track" data set for the western North Pacific, as many as 25 typhoons have passed within 75 km of Kamikoshiki since the beginning of the compilation in 1945 AD (Chu et al., 2002).

The coastline of Kamikoshiki is flanked with large lagoon systems formed by drowned coastal valleys cutoff from the sea by a long gravel bar called Nagame-no-Hama (Aramaki et al., 1969). Lake Namakoike and Lake Kaiike, are the deepest of

Kamikoshiki's coastal lagoons (Fig. 1), with respective surface areas of 0.5 km^2 and 0.15 km^2, and respective maximum depths of 21 m and 10.7 m (Matsuyama, 1977).

Lake Kaiike exhibits a significant chemocline at roughly 2.5 m and remains stratified throughout the year (Matsuyama, 1977; Nakajima et al., 2003). Anoxic bottom waters within the lake prevent bioturbation, and result in well-preserved, fine-scale (<1 mm) sedimentary stratigraphy (Oguri et al., 2002). Modern sedimentation rates in the lake based on Pb-210 analyses are approximately 2.3 mm yr−1 (Kotani et al., 2001), which suggest that sub-millimeter laminations represent depositional processes occurring on the annual-to-subannual timescales. Microscopic observations (Oguri et al., 2003a; Oguri et al., 2002) indicate that micro-laminations are constructed of higher density, diatom-rich layers (Kashima, 1989; Kubo et al., 1999), interbedded with lower density lamina of bacterial species which populate the lake's bottom and chemocline (Koizumi et al., 2004a; Koizumi et al., 2005; Koizumi et al., 2004b; Matsuyama, 2004; Matsuyama and Moon, 1998; Matsuyama and Shirouzu, 1978; Nakajima et al., 2003; Oguri et al., 2004). These previous studies have focused primarily on the upper few centimeters of Lake Kaiike sediment. Less work has been conducted on the lake's long-term depositional history, although sub-bottom seismic profiling using a Uni-boom system reveal over 20 meters of sediment accumulation (Oguri et al., 2002).

Lake Namakoike exhibits less water-column stratification than Lake Kaiike (Matsuyama, 1977); however, recent measurements suggest near meromictic conditions in its deepest reaches, with anoxic sediments similar to Kaiike (Takishita et al., 2007). Both Lake Kaiike and Namakoike have fairly small watersheds, with respective catchments of 0.17 km^2 and 1.5 km^2 (Matsuyama, 1977). The local tidal range at the site is approximately 2 m, but modern tidal flow into both lakes is restricted to seawater seeping through the gravel barrier, resulting in a dampened tidal range of roughly 0.2 m (Aramaki et al., 1969). Heavy precipitation can also increase water levels in Lake Kaiike to the point that no tidal variation is observed, and flow is continuous into Lake Namakoike through a small channel which connects the two lakes (Matsuyama, 1977).

The region surrounding Kamikoshiki is fairly stable tectonically with few active faults in the area (National Astronomical Observatory, 1992; Taira, 2001; Yokoyama et al., 1996). Relative sea-level (RSL) observations for coastal regions of Kyushu are numerous (e.g. Chida, 1987; Moriwaki et al., 1986; Moriwaki et al., 2002; Nagaoka et al., 1991; Nagaoka et al., 1995; Nagaoka et al., 1997a; Nagaoka et al., 1997b; Nakada et al., 1994; Ohira, 2005; Shimoyama, 1994; Shimoyama et al., 1991), with observations from southwestern Kyushu (Nagaoka et al., 1996; Yokoyama et al., 1996) exhibiting little evidence for tectonic activity over the mid-to-late Holocene. Quantitative glacial-isostatic modeling results (Nakada et al., 1991) are consistent with mid-Holocene RSL reconstructions from western Kyushu (Fig. 2), and support sea-level at the Kamikoshiki study area remaining fairly stable over the last 6000 yrs, with the site roughly situated on the nodal point for isostatic adjustment (Fig. 2).

The 2-4 m high gravel bar (Nagame-no-hama) that separates Namakoike and Kaiike from the sea is continuous with no tidal inlets. However, during Typhoon Ruth in 1951 AD, an inlet was opened into the barrier at the north end of Lake Namakoike. The 1951 AD inlet was later repaired with a presently-standing concrete seawall (Fig. 1;

Matsuyama, 1981). Thus, Typhoon Ruth was the last event to occur at the site without known human fortifications of the Nagame-no-hama barrier.

3. Material and methods

To assess the long-term depositional history for Lake Kaiike and Lake Namakoike we obtained high-resolution subbottom seismic data, sediment cores, and geochronologies from both lakes. Sub-bottom seismic surveys were collected in 2006 using an EdgeTech SB-424 chirp seismic system with a 4–24 kHz pulse bandwidth. A uniform sound speed of 1500 m/s was used to convert travel time to depth. Bottom penetration by the chirp unit was sufficient to image the entire stratigraphic sequence of both lakes (~10-20 m) with a vertical resolution of roughly 10 cm. Coring locations were targeted where seismic profiles revealed the longest and most complete depositional sequence from each sedimentary basin. Geographic positions for chirp survey lines and coring sites were obtained using a handheld GPS unit, which provided horizontal accuracies of 3 to 6 m.

Sediment cores were collected using a piston push core system with 5 cm diameter polycarbonate and aluminum barrels (Colinvaux et al., 1999). Cores were collected in 2-3 m drives with 20-30 cm of sediment overlap. Consecutive drives were obtained from alternating sides of the coring platform to prevent sediment disruption at depths where drives overlapped. Additional hand-held gravity cores were collected to obtain surface samples with a well-preserved sediment/water interface.

Sediment cores were shipped to the Woods Hole Oceanographic Institution (WHOI) where they were refrigerated at 4 °C prior to being split, described and photographed. Select core halves were run through a non-destructive, X-ray fluorescence core scanner (XRF) to obtain a high resolution down-core profile (≤1 mm) of the sediment's elemental composition (Croudace et al., 2006), as well as relative density measurements using digital X-ray radiography. Discrete surface samples collected from the watershed and barrier beach were also run through the XRF to identify the elemental composition of allochthonous material in both lakes. All samples were run with a 3 kW Molybdenum (Mo) target tube with a 10 second exposure time. In this study we focus on XRF results for Strontium (Sr), which has a good response for excitation in sediment using a Mo target (Thomson et al., 2006), and is found in high concentrations within the marine sourced shell, coral and algal material often advected into lagoons during overwash events (Bowen, 1956; Woodruff, 2008). Coarse fractions were determined by measuring the weight of dry sand in samples relative to the weight of bulk material, where sands were isolated using a 63 µm sieve after treatment with hydrogen peroxide to remove organics.

Modern sediment chronologies were obtained for surface cores by gamma spectrometry. Measurements for ^{137}Cs (a product of atmospheric nuclear weapons testing) were gathered nondestructively using a high-resolution gamma detector. This anthropogenic radionuclide has been released to the environment predominantly since the early 1950s, the beginning of atmospheric nuclear weapons testing, with fallout reaching a maximum in 1963 AD (Frignani and Langone, 1991; Ritchie and McHenry, 1990). However, the onset of local ^{137}Cs flux to the site could potentially begin as early as 1945 AD due to the WWII atomic bombing of nearby Nagasaki, Japan, located approximately 100 km north of the site (Kudo et al., 1991; Saito-Kokubu et al., 2008). For radioisotope analysis, approximately 2.0 g of powdered sediment samples were placed in 2.54 cm diameter plastic jars and counted on a Canberra GCW4023S coaxial germanium well detector for 24–48 h. Activities for ^{137}Cs were computed spectroscopically from the 661.7 keV photopeak.

Centennial-to-millennial scale chronologies were constrained by Accelerator Mass Spectrometry (AMS) ^{14}C dates of plant material. Samples were gently washed with distilled water, sonicated, dried, and dated at the National Ocean Science Accelerator Mass Spectrometry Facility in Woods Hole, Massachusetts (NOSAMS). Resulting ^{14}C ages were calibrated to calendar years Before Present (yr BP) using IntCal04 (Reimer et al., 2004), where 1950 AD is defined as "Present" by convention.

4. Results

4.1 Seismic data

Chirp surveys of Lake Namakoike and Lake Kaiike reveal similar subbottom stratigraphy. Both lakes contain approximately 10-15 meters of acoustically laminated sediment lying over a reflective bedrock surface (Fig. 3). Lake Namakoike exhibits multiple subaqueous bedrock ridges that partition the lake into at least four separate submerged basins. Similar top sediments within Namaikoike depocenters consist of acoustically laminated, parallel to subparallel seismic reflectors that are generally thickest in the middle of each basin and convergent along the edges of adjacent bedrock ridges (Fig. 3).

A mainly depositional sequence within the upper-most sedimentary unit (Unit 1) drapes an erosional incision at a sediment depth of approximately 3-to-4 m (Fig. 3). Stratigraphic signatures of substantial erosion are evident below this contact surface, and include truncated stratigraphy and cut/fill features. The northern most basin surveyed in Namakoike (Basin-NA, located directly next to the Nagame-no-hama seawall), contains truncated unconformities at the base of Unit 1, which suggest downcutting of at least 1-to-2 m (Fig. 3). The truncated strata below Unit 1 at the Nagame-no-hama seawall provide evidence for additional barrier openings prior to Typhoon Ruth in 1951 AD, and suggest this stretch of the barrier is a hotspot for breaching. In comparison, Basin-NB (located just to the south of Basin-NA, Fig. 3) contains less evidence of channel incisions and/or sediment redistribution. Preservation of strata within Basin-NB may be due to the submerged ridge separating it from Basin-NA, which provides some shelter against erosion when the barrier is compromised along the more vulnerable stretch of coast adjacent to Basin-NA.

Chirp surveys from Lake Kaiike are similar to those collected from Lake Namakoike, exhibiting a top unit of parallel laminations (Unit 1), draped over a lower unit with truncated reflectors and more complicated stratigraphy (Fig. 3). These observations are also consistent with previous Uni-boom data collected from Kaiike (Oguri et al. (2003b), that identified an acoustically conductive 2-3 m thick top unit, overlying a second unit with slightly higher levels of acoustical impedance.

4.2 Sedimentology

The parallel and undisturbed stratigraphy in Unit 1 suggests a fairly complete sedimentary sequence within this upper unit (Fig. 3). In addition, Basin-NB appears to contain the most expanded record for Unit 1, with the least evidence for sediment disruption along the erosional contact at its base. Based on these stratigraphic observations we focus our initial sedimentological analyses on NKI5, a 5.5 m core collected from the middle of Basin-NB (core location identified in Figs. 1 and 3).

NKI5 is primarily composed of organic-rich, finely-laminated mud, intercalated with coarser grained deposits. Depth profiles of percent coarse and x-ray gray-scale density indicate the depths for coarse beds are concurrent with prominent seismic reflectors (Fig. 4). In particular, the deposit concomitant with the erosional surface at the base of Unit 1 is distinct, containing the highest sand content observed in NKI5 (~50%). Coarse deposits generally consist of rounded sand-to-pebble sized siliciclastic grains, interspersed with calcium carbonate shells and shell fragments. These coarse beds are low in organic material, and well mixed, with an absence of internal, fine-scale laminations. In comparison, deposits of lower acoustical impedance situated between coarser grained deposits are 10-30 times finer grained, with preserved fine-scale laminae (<1 mm), and contain considerably more organic detritus.

Concentrations of Sr are approximately 4 times larger for discrete sandy surface samples collected along the subaerial portions of the Nageme-no-hama barrier (2075 ± 950 int. peak area, 2σ) compared to the coarse subaerial sediment samples collected from the watershed and small tributaries which feed Lake Namakoike and Lake Kaiike (500 ± 120 int., 2σ). The coarse, rounded, siliciclastic grains within NKI5 deposits and high Sr concentrations within these sediments are therefore both characteristic of reworked sand and shell material derived from the site's barrier beach, rather than coarse sediment carried into the lagoon from the watershed during high runoff events (Fig. 4). Higher-resolution analyses of the upper 50 cm of NKI5 also show similar trends, with smaller peaks in percent coarse correlated to more subtle increases in Sr (Fig. 5). Sediments low in Sr are generally finer grained with sub-millimeter laminations (Figs 4 and 5). These characteristics suggest that this finely-laminated sediment is deposited under quiescent conditions associated with a highly stratified water column, anoxic bottom waters, and low bioturbation.

4.3 Geochronology

The 1963 AD ^{137}Cs peak in NKI5 occurs at roughly 10 cm (Fig. 5), indicating sedimentation rates of roughly 2.3 mm/yr since 1963 AD. This ^{137}Cs peak also occurs just above the most recent deposit in NKI5, between 12 and 16 cm (Fig. 5) suggesting this coarser layer was deposited in the 1950's, and likely by the typhoon breach to the Nagame-no-hama barrier in 1951 AD.

Radiocarbon ages in both cores increase monotonically with sediment depth indicating fairly steady long-term sedimentation rates in both cores, with the exception of a ~1500 year step-function increase in age at roughly 420 cm in NKI5 (Fig. 6 and Table 1). The depth of this hiatus is at the base of Unit 1 (Fig. 4), and is consistent with truncated strata indicating downcutting of sediment below this layer (Fig. 3). An additional step-function increase in age may also occur between 212 and 259 cm in NKI5 (Fig. 6). However, evidence for erosion is less apparent in the seismic profiles between these two depths (Fig. 4).

In general, sedimentation rates are slightly lower in KI2 than in NKI5 (Fig. 6). This is consistent with chirp surveys indicating a slightly more condensed stratigraphy in Lake Kaike relative to Basin-NB in Namakoike (Fig. 3). The sedimentation rates for both cores increase towards the modern, and become roughly equal at approximately 400 yr BP (Fig. 6). These results are also consistent with the ^{137}Cs measurements for NKI5, and ^{210}Pb analyses of sediment collected near KI2 (Kotani et al., 2001), both of which show sedimentation rates of approximately 2.3 mm/yr for historical sediments.

Sedimentological analyses of NKI5 and discrete surface samples collected from the Nagame-no-hama barrier indicate Sr as a reasonable indicator of seaward-sourced, coarse grained material. The timing of Sr peaks are also similar in NKI5 and KI2, suggesting both lakes have experienced congruent periods of marine inundation (Fig. 7). For instance, deposits high in Sr are evident at both sites between approximately 3600 and 2500 yr BP. Following this period, an interval of lower Sr levels indicates more quiescent conditions within both lakes. Evidence for another active period for marine influence begins at roughly 1000 yr BP, and generally lower Sr concentrations are evident in both lakes between about 300 yr BP (1650 A.D.) and present.

5. Discussion

5.1 Barrier morphodynamics

The temporal correlation between deposits in lakes Namakoike and Kaiike indicates coherence between the two systems (Fig. 7), either by exchange through the small channel which connects them or by multiple concurrent breaches through the Nagame-no-hama barrier. Seismic data collected next to the small channel connecting the two lakes did not show any evidence of substantial incision into the bedrock ridge partitioning the two systems, an indication that the channel has never been significantly deeper than its current depth of less than 1 m. On the basis of these seismic observations it appears unlikely that flow through the channel was great enough to produce the erosional stratigraphy observed in both lakes (Fig. 3). The concurrent marine deposits observed in Lake Kaiike and Lake Namakoike are therefore likely due to multiple breaches through the Nageme-no-hama barrier during roughly the same time interval.

The preserved, finely laminated sediments at the base of core NKI5 dating to between 6200 and 5100 yrs BP likely indicate stratified, anoxic bottom waters in Namakoike during this interval, thus preventing bioturbation (Fig. 7). This is with the exception of a minor disruption in laminae at ~470 cm or ~5500 yr BP. The barrier adjacent to Namakoike was therefore likely subaerial by 6200 yr BP (Fig. 7), since the barrier shelters the lake from waves, and the mixing of fresh, oxygenated seawater down to the bottom of the basin.

Comparing Sr depth profiles for cores NKI5 and KI2 shows concentrations of Sr are generally lower in KI2 than in NKI5 (Fig. 7), a pattern consistent with the slightly more sheltered location of Lake Kaiike within the northern embayment of Kamikoshiki (Fig. 1). The coarse-deposits intercalated within the finely-laminated sediments of Kaiike and Namakoiike show a gradual decrease in both Sr concentrations and grain-size up-core (Fig. 4 and 7). These reductions may indicate periods of inundation over the Nagame-no-hama barrier have become less severe through time, a result consistent with initial descriptions for the gradual development of the barrier over the last few millennia (Aramaki et al., 1969).

It is possible that the Nagame-no-hama barrier formed with the emergence of an ancient submerged bar, in response to a general fall in relative sea level following a mid-Holocene highstand (Aramaki et al., 1969). Most coastal regions of Japan show evidence for sea levels several meters above present day during an interval ranging between roughly 6500 and 5000 years BP (e.g. Ota and Machida, 1987), examples include; locations along the eastern coast of Hokkaido (Maeda et al., 1992; Sawai, 2001), at the southern Boso Peninsula and along Sagami Bay (Endo et al., 1982; Kumaki, 1985;

Nakata et al., 1980), in coastal regions of western Kobe (Sato et al., 2001), and along the Ryukyu Island of Kikai-jima (Sugihara et al., 2003; Webster et al., 1998). However, regional glacial-isostatic modeling results (Nakada et al., 1994; Nakada et al., 1991) and RSL reconstructions (Nagaoka et al., 1996; Yokoyama et al., 1996) from the more tectonically stable areas of western Kyushu (Taira, 2001) provide evidence that sea-level has remained fairly constant at Kamikoshiki over the last 6000 years (Fig. 2). If this is the case, the decrease in both grain-size and Sr within successive deposits in both NKI5 and KI2 indicate that under steady sea-level conditions the barrier has gradually become less susceptible to inundation, likely becoming more fortified through time by mechanisms other than changes in relative sea-level (e.g. longshore transport (e.g. Hine, 1979), overwash and backbarrier deposition (e.g. Morton, 2002), and/or vegetative growth (e.g. Snyder and Boss, 2002)).

The multiple deposits in both NKI5 and KI2 strongly suggest that the barrier has been breached numerous times over the last 6400 years, with finely-laminated sediments between these deposits indicating that each of these breaches has closed naturally following the event. Several peaks in both Sr and grain-size are also observed within unlaminated coarser grained units (Fig. 4 and Fig. 7), which may suggest deposition by multiple events. The barrier is likely more susceptible to overwash after an initial breach and following vegetative disruption (Morris et al., 2001; Morton and Paine, 1985; Stockdon et al., 2007; White, 1979). Successive severe flooding events therefore may serve to maintain the breach opening over time. It is unclear what stimulates the refortification of the barrier and the restoration of meromictic conditions in both lakes. While some overwash by smaller flooding events is necessary to elevate subaerial portions of the barrier (Stone et al., 2004), it is likely that inlet closure occurs in general during periods of less extreme flooding, which would allow reestablishment of the Nagame-no-hama barrier without severe and repetitive disruptions.

5.2 Deposit origins

Both tropical cyclones and tsunamis have the ability to inundate barrier beach systems and produce coarse deposits comparable to those observed at the site. Well documented tsunami deposits are evident along the Japanese coast. However, these deposits are primarily observed to the north of Kamikoshiki and closer to subduction/collision plate boundaries; e.g. along the Pacific Ocean facing shorelines of Hokkaido (Nanayama et al., 2007; Nanayama et al., 2003; Sawai, 2002), Honshu (Fujiwara and Kamataki, 2007; Komatsubara and Fujiwara, 2007; Sawai et al., 2008) and Shikoku (Okamura et al., 1997; Okamura et al., 2000; Okamura et al., 2003), as well as some coastal regions in the Japan Sea (e.g. Nanayama and Shigeno, 2006). Evidence for tsunamis are less prevalent along the more tectonically stable regions of western Kyushu, . This is with the exception of documented tsunamis in Ariake Bay near Nagasaki and along the north side of Kagoshima Bay, where significant wave runup were constrained predominantly to the local embayments near the point of initiation (Watanabe, 1998)).

Another seismically active region of Japan with tsunami potential is located to the south of the site along the Ryukyu Trench (Taira, 2001). On April 24, 1771 AD, a very large tsunami struck the Ryukyu Islands, located approximately 1000 km to the south of Kamikoshiki. Large coral boulders located the eastern shore of the Ryukyu Islands have been attributed to this event (Kawana and Nakata, 1994). However, recent work by Suzuki et al. (2008) shows a fairly wide range of ^{14}C ages for the timing of transport of these boulders. In addition, oxygen isotope micro-profiling and skeletal growth patterns reveal that these coral blocks were likely dislodged and transported primarily during the tropical cyclone season, and not in the spring during the 1771 AD tsunami.

Tsunamis cannot be explicitly ruled out as a cause for the deposits observed in Namakoike and Kaiike. However, only one minor tsunami events has been documented on the island since 1945 AD (Japan Meteorological Agency, 2007; National Geophysical Data Center, 2009), compared to the 25 typhoons which have passed within 75 km of Kamikoshiki during this interval (Chu et al., 2002). This tsunami occurred in response to the 1960 Chilean Earthquake with a recorded wave height of only ~0.8 m on the island, (compared to wave heights which reached a maximum of roughly 8.0 m during the event along the shorelines of Japan which directly facing the Pacific Ocean (National Geophysical Data Center, 2009)).

In addition to the best track data set, the island also has a much longer written history of typhoons including multiple tropical cyclone strikes between 1883-1886 AD, which resulted in wide-spread starvation on Kamikoshiki, and the relocation of its residents to the island of Tanega-shima, Japan (Inomoto, 1999). A monument found in Nishinoomote city on Tanega-shima commemorates the 100th anniversary of this settlement, and reads:

> 明治十六年より三か年に亘り甑島に襲来せる台風の言語に絶する惨状を機に出郷せし十九戸が明治十九年四月十五日この地に移住…

translating to:

As a result of the indescribable disaster caused by three consecutive years of typhoons that hit Koshiki-jima since 1883, 19 families left their homes to settle in this area on April 15, 1886…

Similar to instrumental observation, no documentation exists for any significant tsunami event at Kamikoshiki within the recent historical record (Watanabe, 1998). Therefore, the lack of any significant tsunami events at Kamikoshiki and the high likelihood of typhoon strikes to the site, both strongly suggest that a majority of breaches to the Nagame-no-hama barrier are due to tropical cyclones.

5.3 Comparison with El Niño/Southern Oscillation proxies

Since 1945 AD, studies using instrumental observations indicate that the El Niño/Southern Oscillation (ENSO) has had a significant influence on tropical cyclone activity (e.g. Trenberth et al., 2007). In the western North Atlantic there is a general suppression of hurricane genesis during El Niño years (Bove et al., 1998; Gray, 1984) . Conversely, the overall frequency of tropical cyclone occurrences is less affected by ENSO variability in the western North Pacific (Elsner and Liu, 2003). However, there is a marked eastward shift in genesis location during El Niño years (Chan, 1985; Lander, 1994). Typhoons also tend to become more intense during El Niño events (Camargo and

Sobel, 2005), and have frequent recurving trajectories which may result in a higher likelihood of tropical cyclone strikes along Japan and Korea (Elsner and Liu, 2003).

In order to evaluate the role of ENSO in governing typhoon activity over the mid-to-late Holocene, we compare patterns of typhoon-induced deposition at Kamikoshiki to an annually resolved El Niño proxy reconstruction from Laguna Pallacocha, Ecuador (Moy et al., 2002). The Laguna Pallacocha proxy is based upon clastic sediments that wash into the lake during heavy rains that occur predominantly during moderate-to-strong El Niño events. Additional proxy records of ENSO variability are also available (e.g. Cobb et al., 2003; D'Arrigo et al., 2005; Lachniet et al., 2004; Stahle et al., 1998). However, to date the Pallococha record is still the only complete, high-resolution record which exists for the mid-to-late Holocene. In addition, a strong correspondence occurs over the past two millennia between the Pallacocha record and ENSO reconstructions using stalagmite $\delta^{18}O$ records from Isthmus of Panama (Lachniet et al., 2004), providing further support for the Pallacocha record as an accurate reconstruction of Holocene El Niño-like variability.

Comparisons between the Kamikoshiki and Pallacocha records show a general correlation between periods of increased El Niño occurrence and periods of more typhoon-induced deposition at the study site (Fig. 8). For example, marine deposits in Namakoike and Kaiike between 300-to-1000 yr BP, 2500-to-3600 yr BP, and 4300-to-4800 yr BP are roughly concurrent with periods of more El Niño activity. In contrast, laminated meromictic sediments which likely reflect more quiescence conditions in both lakes (present-to-300 yr BP, 1200-to-2200 yr BP, 3600-to-4300 yr BP, and 5200-to-6400 yr BP) occur generally during intervals of less El Niño activity. Therefore, similar to some studies using instrumental and historical observations (Elsner and Liu, 2003; Fogarty et al., 2006; Wang and Chan, 2002), the millennial-scale reconstructions from both Namakoike and Kaiike support a pattern of more typhoon strikes to southern Japan during El Niño years.

5.4 Comparison with global and regional tropical cyclone reconstructions

On average, approximately 90 tropical storms develop each year globally (Emanuel, 2006; Henderson-Sellers et al., 1998). This number is remarkably stable with a standard deviation of only about 10, compared to local regional variations in tropical storm counts which are typically 100% of the long-term mean (Henderson-Sellers et al., 1998). It is currently unclear why the total number of tropical storms occurring globally remains fairly stable while regional variations are so high (Emanuel, 2006), or whether this relationship existed prior to the satellite era.

Tropical cyclone reconstructions from the western North Atlantic suggest significant hurricane variability on the centennial-to-millenial timescales (Donnelly and Woodruff, 2007; Scileppi and Donnelly, 2007; Woodruff et al., 2008a). Comparisons between the Kamikoshiki typhoon reconstruction and these hurricane proxy records suggest an inverse relationship. For instance, overwash trends within the Laguna Playa Grande reconstruction from Vieques, Puerto Rico are similar to additional reconstructions from the western North Atlantic and likely represent basin wide variations in hurricane activity (Donnelly and Woodruff, 2007; Woodruff et al., 2008a). Increased overwash activity observed in Namakoike and Kaiike between roughly 3600-to-2500 yrs BP, and 1000-to-300 yrs BP generally occurs during periods of less overwash activity at Laguna Playa Grande (Fig. 8). In contrast, the quiescence conditions in both of the Kamikoshiki lakes between roughly 300 yr BP-to-present, 2500-to-1000 yrs BP and 3600-to-4300 yrs BP are concurrent with periods of increased hurricane overwash at Laguna Playa Grande.

The inverse correlation between tropical cyclone reconstructions from the western North Atlantic and Kamikoshiki may indicate an oscillating pattern in tropical cyclone activity between the western North Atlantic and western North Pacific on the centennial-to-millenial time-scales, although on shorter time-scales this relationship is less apparent (e.g. Wang and Chan, 2002). The scarcity of millennial scale typhoon reconstructions also makes it difficult to determine whether trends in the Kamikoshiki records reflect basin wide variations in activity or regional shifts in the preferred paths for typhoons.

Observations since 1945 AD suggest ENSO may drive a seesaw pattern in typhoon activity in the western North Pacific, with a general steering of typhoons towards southern Japan during El Niño years and southern China during La Niña years (Chan, 1985). Documented typhoon landfalls to the Guangdong Providence also exhibit an inverse correlation to ENSO over the last few centuries, with a decrease in typhoon occurrences to the Guangdong Providence during strong El Niño years and an increase during strong La Niña years (Elsner and Liu, 2003). Guangdong typhoon and ENSO proxy records were not compared prior to 1600 AD because of a rapid drop in the number of documented typhoon landfalls preceding this date. It is likely that this decrease in typhoon counts is largely an artifact of the undercounting of events within the earlier part of the Guangdong record. However, an additional drop in typhoon landfalls is also observed within the more reliable part of the reconstruction between 1600 and 1650 AD (Fig. 9). Rates of typhoon occurrences following 1650 AD (or 300 yr BP) rise to some of the highest values in the Guangdong reconstruction. This transition to more documented typhoon activity in Guangdong at ~300 yr BP is concurrent with the most recent drop in Sr concentrations within NKI5 (Fig. 9). A subtler decrease in Sr at this time is also evident in KI2. The concurrent transition to more quiescent conditions in both Namakoike and Kaike during the rapid increases in Guangdong typhoon counts at 300 yr BP may suggest an oscillation in tropical cyclone activity between southern China and southern Japan, an observation consistent with ENSO-driven variability in typhoon tracks.

5.5 Comparison with historical record of Japanese typhoons

Historical accounts from Kamikoshiki Island, although incomplete, begin in 769 AD (Shoku-Nihongi, 797) and include the description of a series of devastating typhoon strikes to the island between 1883 AD and 1886 AD (Inomoto, 1999). Following these events most residents emigrated from Kamikoshiki due to crop destruction and the termination of ferry service to and from the island. The timing for the event layer at 35 cm in NKI5 is slightly older than 1883 AD (Fig. 5, assuming a steady sedimentation rate derived from the 1963 AD ^{137}Cs peak), but may still be associated with the 1883-1886 AD typhoons given the margin of error in extrapolating recent ^{137}Cs sedimentation rates to older sediments.

In addition to the more recent 1883-1886 AD events, two famous typhoons also made landfall to the north of Kamikoshiki at the end of the 13th century. These timely storms are cited as contributing to the failed Mongol invasions in 1274 AD and 1281 AD, with respective armadas including 30,000 and 140,000 men (Hall, 1971). Temples and shrines at the time famously identified these tropical cyclones as “divine wind” or *kamikaze*, signifying their importance in maintaining Japanese sovereignty (Emanuel, 2005). Detailed observations are limited for these two early typhoons; however, it is likely that they passed just to the east of the study site before making landfall approximately 200 km to the north along the Kyushu mainland (Hall, 1971). A rather large Sr peak in NKI5 dates to approximately 1300 AD (Fig. 9), and is roughly concurrent with the timing for the *Kamikaze* typhoons (given ^{14}C dating uncertainties). A similar Sr spike is not evident in KI2 (Fig. 9). Therefore, more detailed chronologies from additional Kamikoshiki sediments are required in order to verify the 1300 A.D. deposit. Nonetheless, the two *Kamikaze* storms do appear to have occurred during a period with more frequent marine-sourced deposition at the site (Fig. 9).

6. Conclusions

We provide a 6400 year record of episodic coastal flooding using sediment deposits from two coastal lakes located on the remote island of Kamikoshiki in southwestern Japan. The timing of marine-flood deposits is replicated in both lakes and provides evidence for multiple coastline breaches into the two basins during periods of frequent marine inundation. Preservation of laminated sediments between marine flood deposits indicates similar quiescent intervals in both lakes, likely due to a lack of overwash events. A deposit dating to the mid-20th century is consistent with a documented breach to the barrier during a typhoon in 1951 AD. This modern analog, in combination with the high frequency of typhoon strikes to the site and the absence of significant historic tsunamis, lead us to conclude that marine flood deposits are likely the result of tropical cyclones. Active breaching intervals at Kamikoshiki are concurrent with; 1) periods of more frequent El Niño events, and 2) periods of lower hurricane activity in the western North Atlantic. This pattern is consistent with instrumental observations which indicate that during El Niño years more typhoons are steered towards Japan, while hurricane activity is generally suppressed in the western North Atlantic.

Decreases in marine-sourced deposition at Kamikoshiki starting around 300 yr BP occur during a transition to more documented typhoon strikes in the Guangdong Providence of southern China, a pattern that is consistent with potential centennial-to-millennial scale changes in the preferred tracks for typhoons in response to ENSO variability. Failed Mongol invasions of Japan during the late 13th century occur during a period of more frequent marine-sourced deposition at the site, which may indicate that the invasions took place during a period of greater typhoon activity for southern Japan.

7. Acknowledgements

The authors would like to specially thank M. Okusu, F. Woodruff, and J.W. Woodruff who helped conduct the field work for this study. We are also grateful to K. Oguri, S. Hirano, K. Kashima, and F. Nanayama for providing valuable insight and a compilation of background literature. M. Gomes, R. Sorell and J. Tierney assisted with laboratory analyses. C. Saenger and P. Lane provided thoughtful comments on the manuscript and H. Okusu helped with the translation of Japanese documents. The study was supported by the Coastal Ocean Institute(COI) and the Ocean and Climate Change Institute(OCCI) at Woods Hole Oceanographic Institute. This article benefited through constructive reviews by two anonymous referees. We dedicated this paper to the memory of Makoto Ohkusu.

8. References

Arakawa, H., Ishida, Y., and Ito, T. (1961). "Historical documents of storm surges in Japan." Meteorological Research Institute.

Aramaki, M., Yamaguchi, M., and Tanaka, Y. (1969). A geomorphological and hydrological study on lagoons of kamikoshiki islands. *Japan, Senshu-Shizenkagaku-Kiyo* **9,** 1-80.

Besonen, M. R., Bradley, R. S., Mudelsee, M., Abbott, M. B., and Francus, P. (2008). A 1,000-year, annually-resolved record of hurricane activity from Boston, Massachusetts. *Geophysical Research Letters* **35**.

Bove, M. C., Elsner, J. B., Landsea, C. W., Niu, X. F., and O'Brien, J. J. (1998). Effect of El Nino on US landfalling hurricanes, revisited. *Bulletin of the American Meteorological Society* **79,** 2477-2482.

Bowen, H. J. M. (1956). Strontium and barium in seawater and marine organisms: Jour. *Marine Biol. Assoc. United Kingdom* **35,** 451-460.

Buynevich, I. V., FitzGerald, D. M., and Goble, R. J. (2007). A 1500 yr record of North Atlantic storm activity based on optically dated relict beach scarps. *Geology* **35,** 543-546.

Camargo, S. J., and Sobel, A. H. (2005). Western North Pacific Tropical Cyclone Intensity and ENSO. *Journal of Climate* **18,** 2996-3006.

Chan, J. C. L. (1985). Tropical Cyclone Activity in the Northwest Pacific in Relation to the El Niño/Southern Oscillation Phenomenon. *Monthly Weather Review* **113,** 599-606.

Chan, J. C. L. (2007). Interannual variations of intense typhoon activity. *Tellus A* **59,** 455-460.

Chan, J. C. L., and Shi, J. (2000). Frequency of typhoon landfall over Guangdong Province of China during the period 1470–1931. *Int. J. Climatol* **20,** 183-190.

Chida, N. (1987). Holocene geomorphic development in the western Ooita Plains. *Geographical Review of Japan* **60A,** 466-480 (In Japanese).

Chu, J.-H., Sampson, C. R., Levine, A. S., and Fukada, E. (2002). The Joint Typhoon Warning Center tropical cyclone best-tracks, 1945-2000 (N. R. Lab., Ed.), Washington, D.C.

Cobb, K. M., Charles, C. D., Cheng, H., and Edwards, R. L. (2003). El Niño/Southern Oscillation and tropical Pacific climate during the last millennium. *Nature* **424,** 271-276.

Colinvaux, P., De Oliveira, P. E., and P., M. (1999). "Amazon pollen manual and atlas." Hardwood Acad. Publ., Amsterdam, Netherlands (NLD).

Croudace, I. W., Rindby, A., and Rothwell, R. G. (2006). "ITRAX: description and evaluation of a new multi-function X-ray core scanner." Geological Society, London.

D'Arrigo, R., Cook, E. R., Wilson, R. J., Allan, R., and Mann, M. E. (2005). On the variability of ENSO over the past six centuries. *Geophys. Res. Lett* **32**.

Donnelly, J. P. (2005). Evidence of past intense tropical cyclones from backbarrier salt pond sediments: A case study from Isla de Culebrita, Puerto Rico, USA. *Journal of Coastal Research***,** 201-210.

Donnelly, J. P., Bryant, S. S., Butler, J., Dowling, J., Fan, L., Hausmann, N., Newby, P., Shuman, B., Stern, J., Westover, K., and Webb, T. (2001a). 700 yr sedimentary record of intense hurricane landfalls in southern New England. *Geological Society of America Bulletin* **113,** 714-727.

Donnelly, J. P., Butler, J., Roll, S., Wengren, M., and Webb, T. (2004). A backbarrier overwash record of intense storms from Brigantine, New Jersey. *Marine Geology* **210,** 107-121.

Donnelly, J. P., and Giosan, L. (2008). Tempestuous highs and lows in the Gulf of Mexico. *Geology* **36,** 751-752.

Donnelly, J. P., Roll, S., Wengren, M., Butler, J., Lederer, R., and Webb, T. (2001b). Sedimentary evidence of intense hurricane strikes from New Jersey. *Geology* **29,** 615-618.

Donnelly, J. P., and Webb, T. (2004). Back-barrier Sedimentary Records of Intense Hurricane Landfalls in the Northeastern United States. *In* "Hurricanes and Typhoons: Past, Present and Future." (R. Murnane, and K. B. Liu, Eds.), pp. 58-95. Columbia University Press, New York City.

Donnelly, J. P., and Woodruff, J. D. (2007). Intense hurricane activity over the past 5,000 years controlled by El Niño and the West African monsoon. *Nature* **447,** 465-468.

Duke, W. L. (1985). Hummocky cross-stratification, tropical hurricanes, and intense winter storms. *Sedimentology* **32,** 167-194.

Elsner, J. B., and Liu, K. B. (2003). Examining the ENSO-typhoon hypothesis. *Climate Research* **25,** 43-54.

Emanuel, K. (2006). Climate and tropical cyclone activity: A new model downscaling approach. *Journal of Climate* **19,** 4797-4802.

Emanuel, K. A. (2005). "Divine Wind: The History and Science of Hurricanes." Oxford University Press, USA.

Emery, K. O. (1969). "A coastal pond studied by oceanographic methods." American Elsevier Publishing, New York.

Endo, K., Sekimoto, K., and Takano, T. (1982). Holocene stratigraphy and paleoenvironments in the Kanto Plain, in relation to the Jomon Transgression, pp. 1-16.

Fogarty, E. A., Elsner, J. B., Jagger, T. H., Liu, K., and Louie, K. (2006). Variations in typhoon landfalls over China. *Advances in Atmospheric Sciences* **23,** 665-677.

Frappier, A., Knutson, T., Liu, K. B., and Emanuel, K. (2007a). Perspective: coordinating paleoclimate research on tropical cyclones with hurricane-climate theory and modelling. *Tellus Series a-Dynamic Meteorology and Oceanography* **59,** 529-537.

Frappier, A. B., Sahagian, D., Carpenter, S. J., Gonzalez, L. A., and Frappier, B. R. (2007b). Stalagmite stable isotope record of recent tropical cyclone events. *Geology* **35,** 111-114.

Frignani, M., and Langone, L. (1991). Accumulation Rates and 137 Cs Distribution In Sediments Off the Po River Delta and the Emilia-Romagna Coast(Northwestern Adriatic Sea, Italy). *Continental Shelf Research* **11**.

Fujiwara, O., and Kamataki, T. (2007). Identification of tsunami deposits considering the tsunami waveform: An example of subaqueous tsunami deposits in Holocene shallow bay on southern Boso Peninsula, Central Japan. *Sedimentary Geology* **200,** 295-313.

Goldenberg, S. B., and Shapiro, L. J. (1996). Physical mechanisms for the association of El Nino and west African rainfall with Atlantic major hurricane activity. *Journal of Climate* **9,** 1169-1187.

Gray, W. M. (1968). Global view of the origin of tropical disturbances and storms. *Monthly Weather Review* **96,** 669-700.

Gray, W. M. (1984). Atlantic Seasonal Hurricane Frequency. Part I: El Nino and 30 mb Quasi-Biennial Oscillation Influences. *Monthly Weather Review* **112,** 1649-1668.

Grossman, M. J. (2001). Large floods and climatic change during the Holocene on the Ara River, Central Japan. *Geomorphology* **39,** 21-37.

Grossman, M. J., and Zaiki, M. (2007). Reconstructing typhoon landfalls in Japan using historical documents: 1801-1830. *Papers and Proceedings of Applied Geography Conferences* **30,** 334-343.

Hall, J. W. (1971). "Japan: From Prehistory to Modern Times." Charles E. Tuttle Co., Tokyo, Japan.

Henderson-Sellers, A., Zhang, H., Berz, G., Emanuel, K., Gray, W., Landsea, C., Holland, G., Lighthill, J., Shieh, S. L., Webster, P., and McGuffie, K. (1998). Tropical cyclones and global climate change: A post-IPCC assessment. *Bulletin of the American Meteorological Society* **79,** 19-38.

Hine, A. C. (1979). Mechanisms of berm development and resulting beach growth along a barrier spit complex. *Sedimentology* **26,** 333-351.

Inomoto, M. (1999). "Tanegashima." Shun'endo Publishing, Kagoshima, Japan.

Ito, M., Ishigaki, A., Nishikawa, T., and Saito, T. (2001). Temporal variation in the wavelength of hummocky cross-stratification: Implications for storm intensity through Mesozoic and Cenozoic. *Geology* **29,** 87-89.

JapanMeteorologicalAgency. (2007). Confirmed Japanese Tsunami Records, Technical Report No. 8. Japan Meteorological Agency, Tokyo, Japan.

Kashima, K. (1989). The distribution patterns of diatoms and the sedimentary process of the diatom valves in the brackish lakes at the Kamikoshiki Island, Kagoshima Prefecture, South Japan. *Jpn J Benthos Res* **35,** 29–40.

Kawana, T., and Nakata, T. (1994). Timing of Late Holocene tsunamis originating around the Southern Ryukyu Islands, Japan, deduced from coralline tsunami deposits. *Japanese Journal of Geography* **103,** 352-376 (In Japanese).

Keen, T. R., Bentley, S. J., Vaughan, W. C., and Blain, C. A. (2004). The generation and preservation of multiple hurricane beds in the northern Gulf of Mexico. *Marine Geology* **210,** 79-105.

Keen, T. R., Furukawa, Y., Bentley, S. J., Slingerland, R. L., Teague, W. J., Dykes, J. D., and Rowley, C. D. (2006). Geological and oceanographic perspectives on event bed formation during Hurricane Katrina. *Geophysical Research Letters* **33, -**.

Koizumi, Y., Kojima, H., and Fukui, M. (2004a). Dominant microbial composition and its vertical distribution in saline meromictic lake kaiike (Japan) as revealed by quantitative oligonucleotide probe membrane hybridization. *Applied and Environmental Microbiology* **70,** 4930-4940.

Koizumi, Y., Kojima, H., and Fukui, M. (2005). Potential sulfur metabolisms and associated bacteria within anoxic surface sediment from saline meromictic Lake Kaiike (Japan). *Fems Microbiology Ecology* **52,** 297-305.

Koizumi, Y., Kojima, H., Oguri, K., Kitazato, H., and Fukui, M. (2004b). Vertical and temporal shifts in microbial communities in the water column and sediment of saline meromictic Lake Kaiike (Japan), as determined by a 16S rDNA-based analysis, and related to physicochemical gradients. *Environmental Microbiology* **6,** 622-637.

Komatsubara, J., and Fujiwara, O. (2007). Overview of Holocene Tsunami Deposits along the Nankai, Suruga, and Sagami Troughs, Southwest Japan. *Pure and Applied Geophysics* **164,** 493-507.

Kotani, T., Ozaki, M., Matsuoka, K., Snell, T. W., and Hagiwara, A. (2001). Reproductive isolation among geographically and temporally isolated marine Brachionus strains. *Hydrobiologia* **446,** 283-290.

Kubo, N., Sawai, Y., and Kashima, K. (1999). Water environment of the coastal brackish lakes in Kamikoshiki Island, Kagoshima Prefecture, Japan. *Laguna* **6,** 261-271.

Kudo, A., Mahara, Y., Santry, D. C., Miyahara, S., and Garrec, J. P. (1991). Geographical distribution of fractionated local fallout from the Nagasaki A-Bomb. *J. Environ. Radioact* **14,** 305-316.

Kumaki, Y. (1985). The deformations of Holocene marine terraces in southern Kanto, Central Japan. *Geogr. Rev. Japan* **58,** 49-60.

Lachniet, M. S., Burns, S. J., Piperno, D. R., Asmerom, Y., Polyak, V. J., Moy, C. M., and Christenson, K. (2004). A 1500-year El Nino/Southern Oscillation and rainfall history for the Isthmus of Panama from speleothem calcite. *Journal of Geophysical Research-Atmospheres* **109,** -.

Lambert, W. J., Aharon, P., and Rodriguez, A. B. (2003). An Assessment of the Late Holocene Record of Severe Storm Impacts from Lake Shelby, Alabama. *Transactions-Gulf Coast Association of Geological Societies* **53,** 443.

Lander, M. A. (1994). An Exploratory Analysis of the Relationship between Tropical Storm Formation in the Western North Pacific and Enso. *Monthly Weather Review* **122,** 636-651.

Lee, K., and Hsu, S. I. (1989). Typhoon records from ancient chronicles of Guangdong Province. *Department of Geography Occasional Paper* **98**.

Liu, K.-b., Shen, C., and Louie, K.-s. (2001). A 1,000-year history of typhoon landfalls in Guangdong, southern China, reconstructed from Chinese historical documentary records. *Annals of the Association of American Geographers* **91,** 453-464.

Liu, K. B., and Fearn, M. L. (1993). Lake-Sediment Record of Late Holocene Hurricane Activities from Coastal Alabama. *Geology* **21,** 793-796.

Liu, K. B., and Fearn, M. L. (2000). Reconstruction of prehistoric landfall frequencies of catastrophic hurricanes in northwestern Florida from lake sediment records. *Quaternary Research* **54,** 238-245.

Maeda, Y., Nakada, M., Matsumoto, E., and Matsuda, I. (1992). Crustal tilting derived from holocene sea-level observations along the east coast of Hokkaido in Japan and upper mantle rheology. *Geophysical Research Letters* **19,** 857-860.

Malmquist, D. L. (1997). Oxygen isotopes in cave stalagmites as a proxy record of past tropical cyclone activity. *In* "22nd Conference on Hurricanes and Tropical Meteorology." pp. 393-394. Amer. Met. Soc., Fort Collins.

Matsuyama, M. (1977). Limnological features of Lake Kaiike, a small lake on Kamikoshiki Island, Kagoshima Prefecture, Japan. *Jap. J. Limnol* **38,** 9-18.

Matsuyama, M. (1981). Three Coastal Lakes on Kamikoshiki Island, Kagoshima Prefecture. *Japanese Journal of Limnology* **42**.

Matsuyama, M. (2004). Phylogenic status of a purple sulfur bacterium and its bloom in Lake Kaiike. *Limnology* **5,** 95-101.

Matsuyama, M., and Moon, S. M. (1998). A bloom of low-light-adapted Chromatium sp. *Lake Kaiike. Jpn J Limnol* **59,** 79-85.

Matsuyama, M., and Shirouzu, E. (1978). Importance of photosynthetic sulfur bacteria, Chromatium sp. as an organic matter producer in Lake Kaiike. *Jpn J Limnol* **39,** 103-111.

Miller, D. L., Mora, C. I., Grissino-Mayer, H. D., Mock, C. J., Uhle, M. E., and Sharp, Z. (2006). Tree-ring isotope records of tropical cyclone activity. *Proceedings of the National Academy of Sciences of the United States of America* **103,** 14294-14297.

Moriwaki, H., Machida, H., Hatsumi, Y., and Matsushima, Y. (1986). Phreatomagmatic eruptions affected by postglacial transgression in the northern coastral area of Kagoshima Bay, Southern Kyushu, Japan. *Journal of Geography* **95,** 94-113 (In Japanese).

Moriwaki, H., Matsushima, Y., Machida, H. I. M., and Arai, F. F. O. (2002). Holocene Geomorphic Evolution around the Aira Caldera, South Japan. *Quaternary Research* **41,** 253-268.

Morris, B. D., Davidson, M. A., and Huntley, D. A. (2001). Measurements of the response of a coastal inlet using video monitoring techniques. *Marine Geology* **175,** 251-272.

Morton, R. A. (2002). Factors Controlling Storm Impacts on Coastal Barriers and Beaches—A Preliminary Basis for Near Real-Time Forecasting. *Journal of Coastal Research* **18,** 486-501.

Morton, R. A., and Paine, J. G. (1985). Beach and vegetation-line changes at Galveston Island Texas: Erosion, deposition, and recovery from Hurricane Alicia (G. C. Bureau of Economic Geology, Ed.), pp. 39. University of Texas at Austin, Austin.

Moy, C. M., Seltzer, G. O., Rodbell, D. T., and Anderson, D. M. (2002). Variability of El Nino/Southern Oscillation activity at millennial timescales during the Holocene epoch. *Nature* **420,** 162-165.

Nagaoka, S., Maemoku, H., and Matsushima, Y. (1991). Holocene geomorphic development in the Miyazaki Plain. *Quaternary Research* **30,** 59-78 (in Japanese).

Nagaoka, S., Yokoyama, Y., Maeda, Y., Nakada, M., and Okuno, J. (1995). Holocene marine sediments and sea level change at the Ikiriki archeological site, southern coast of Oomura Bay, Nagasaki, Japan. *Science Bulletin of Faculty of Education, Nagasaki University* **53,** 27-40 (In Japanese).

Nagaoka, S., Yokoyama, Y., Nakada, M., and Maeda, Y. (1996). Holocene sea-level change in the Goto Islands, Japan. *Geographical reports of Tokyo Metropolitan University* **31,** 11-18 (In Japanese).

Nagaoka, S., Yokoyama, Y., Nakada, M., and Maeda, Y. (1997a). Holocene sea level change and underwater Jomon sites in Fukue Island, Goto Islands, Western Japan. *Science Bulletin of Faculty of Education, Nagasaki University* **56,** 1-11 (In Japanese).

Nagaoka, S., Yokoyama, Y., Nakada, M., Maeda, Y., Okuno, J., and Shirai, K. (1997b). Holocene geomorphic development and sea level change in the Tamana Plain, Southeastern Coast of Ariake Bay, Western Japan. *Geographical Review of Japan* **70A,** 287-306 (In Japanese).

Nakada, M., Maeda, Y., Nagaoka, S., Yokoyama, Y., Okuno, J., Matsumoto, E., Matsushima, Y., Sato, H., Matsuda, I., and Sampei, Y. (1994). Glacio-hydro-isostasy and underwater Jomon sites along the west coast of Kyushu, Japan. *The Quat. Res.(Daiyonki-Kenkyu)* **33,** 361-368 (In Japanese).

Nakada, M., Yonekura, N., and Lambeck, K. (1991). Late Pleistocene and Holocene sea-level changes in Japan: implications for tectonic histories and mantle rheology. *Palaeogeography, Palaeoclimatology, Palaeoecology* **85,** 2.

Nakajima, Y., Okada, H., Oguri, K., Suga, H., Kitazato, H., Koizumi, Y., Fukui, M., and Ohkouchi, N. (2003). Distribution of chloropigments in suspended particulate matter and benthic microbial mat of a meromictic lake, Lake Kaiike, Japan. *Environmental Microbiology* **5,** 1103-1110.

Nakata, T., Koba, M., Imaizumi, T., Jo, W. R., Matsumoto, H., and Suganuma, T. (1980). Holocene marine terraces and seismic crustal movements in the southern part of Boso Peninsula, Kanto, Japan. *Geogr. Rev. Japan, Ser. A* **53,** 29–44.

Nanayama, F., Furukawa, R., Shigeno, K., Makino, A., Soeda, Y., and Igarashi, Y. (2007). Nine unusually large tsunami deposits from the past 4000 years at Kiritappu marsh along the southern Kuril Trench. *Sedimentary Geology* **200,** 275-294.

Nanayama, F., Satake, K., Furukawa, R., Shimokawa, K., Atwater, B. F., Shigeno, K., and Yamaki, S. (2003). Unusually large earthquakes inferred from tsunami deposits along the Kuril trench. *Nature* **424,** 660-663.

Nanayama, F., and Shigeno, K. (2006). Inflow and outflow facies from the 1993 tsunami in southwest Hokkaido. *Sedimentary Geology* **187,** 139-158.

National Astronomical Observatory, J. (1992). Rika nenpyou (Chroniological Scientific Tables), pp. 822-854, Maruzen.

NationalGeophysicalDataCenter. (2009). NOAA/WDC Historical Tsunami Database, Retrieved January 3rd, 2009, from http://www.ngdc.noaa.gov/hazard/tsu_db.shtml.

Nott, J. (2004). Palaeotempestology: the study of and implications Review article prehistoric tropical cyclones - a review for hazard assessment. *Environment International* **30,** 433-447.

Nott, J., Haig, J., Neil, H., and Gillieson, D. (2007). Greater frequency variability of landfalling tropical cyclones at centennial compared to seasonal and decadal scales. *Earth and Planetary Science Letters* **255,** 367-372.

Nott, J., and Hayne, M. (2001). High frequency of 'super-cyclones' along the Great Barrier Reef over the past 5,000 years. *Nature* **413,** 508-512.

Oguri, K., Hirano, S., Sakai, S., Nakajima, Y., Suga, H., Sakamoto, T., Koizumi, Y., Fukui, M., and Kitazato, H. (2003a). Formational processes of sedimentary micro-structure in meromictic Lake Kaiike sediments, Japan. *Geochimica Et Cosmochimica Acta* **67,** A348-A348.

Oguri, K., Itou, M., Sakai, S., Hisamitsu, T., Hirano, S., Kitazato, H., Koizumi, Y., Fukui, M., and Taira, A. (2002). A study on anoxic environment in brackish lake, Kaiike, Kagoshima prefecture: A gateway to ocean anoxic events in the Earth history. *In* "Frontier Research on Earth Evolution." pp. 243-247. JAMSTEC, Yokosuka.

Oguri, K., Itou, M., Sakai, S., Hisamitsu, T., Hirano, S., Kitazato, H., Koizumi, Y., Fukui, M., and Taira, A. (2003b). A study on anoxic environment in brackish lake, Kaiike, Kagoshima prefecture: A gateway to ocean anoxic events in the Earth history. *In* "Frontier Research on Earth Evolution." pp. 243-247. JAMSTEC, Yokosuka.

Oguri, K., Sakai, S., Suga, H., Nakajima, Y., Koizumi, Y., Kojima, H., Fukui, M., and Kitazato, H. (2004). Turbidity variations seen at a sediment surface in meromictic Lake Kaiike, Japan. *In* "Frontier Research on Earth Evolution." pp. 1-6. JAMSTEC, Yokosuka.

Ohira, A. (2005). Data of the Relative Sea-level in the Middle Holocene from the Northern Part of the Nobeoka Plain, East Coast of Kyushu. *Memoirs of the Faculty of Education and Culture, Miyazaki University. Natural science* **12,** 9-19.

Okamura, M., Kurimoto, T., and Matsuoka, H. (1997). Coastal and lake deposits as a monitor. *Chikyu Monthly* **19,** 469–473 (In Japanese).

Okamura, M., Matsuoka, H., Tsukuda, E., and Tsuji, Y. (2000). Tectonic movements of recent 10000 years and observations of historical tsunamis based on coastal lake deposits, pp. 162-168 (In Japanese). Chikyu Month. Symp.

Okamura, M., Tsuji, Y., and Miyamoto, T. (2003). Seismic activities along Nankai Trough recorded in coastal lake deposits. *Kaiyo Monthly* **35,** 312–314 (In Japanese).

Ota, Y., and Machida, H. (1987). Quaternary sea-level changes in Japan. *In* "Sea-level Changes." (M. J. Tooley, and I. Shennan, Eds.), pp. 182-224. Blackwell, New York.

Otvos, E. G. (1999). Quaternary Coastal History, Basin Geometry and Assumed Evidence for Hurricane Activity, Northeastern Gulf of Mexico Coastal Plain. *Journal of Coastal Research* **15,** 438-443.

Otvos, E. G. (2002). Discussion of "Prehistoric Landfall Frequencies of Catastrophic Hurricanes…"(Liu and Fearn, 2000). *Quaternary Research* **57,** 425-428.

Qiao, S. X., and Tang, W. Y. (1993). Compilation and research of climatic data from historical records of the Guangzhou area. Guangzhou: Guangdong People's Press.

Reimer, P. J., Baillie, M. G. L., Bard, E., Bayliss, A., Beck, J. W., Bertrand, C. J. H., Blackwell, P. G., Buck, C. E., Burr, G. S., Cutler, K. B., Damon, P. E., Edwards, R. L., Fairbanks, R. G., Friedrich, M., Guilderson, T. P., Hogg, A. G., Hughen, K. A., Kromer, B., McCormac, G., Manning, S., Ramsey, C. B., Reimer, R. W., Remmele, S., Southon, J. R., Stuiver, M., Talamo, S., Taylor, F. W., van der Plicht, J., and Weyhenmeyer, C. E. (2004). IntCal04 terrestrial radiocarbon age calibration, 0-26 cal kyr BP. *Radiocarbon* **46,** 1029-1058.

Ritchie, J. C., and McHenry, J. R. (1990). Application of Radioactive Fallout Cesium-137 for Measuring Soil Erosion and Sediment Accumulation Rates and Patterns: A Review. *Journal of Environmental Quality* **19,** 215.

Saito-Kokubu, Y., Yasuda, K., Magara, M., Miyamoto, Y., Sakurai, S., Usuda, S., Yamazaki, H., Yoshikawa, S., Nagaoka, S., and Mitamura, M. (2008). Depositional records of plutonium and 137Cs released from Nagasaki atomic bomb in sediment of Nishiyama reservoir at Nagasaki. *Journal of Environmental Radioactivity* **99,** 211-217.

Sato, H., Okuno, J., Nakada, M., and Maeda, Y. (2001). Holocene uplift derived from relative sea-level records along the coast of western Kobe, Japan. *Quaternary Science Reviews* **20,** 1459-1474.

Sawai, Y. (2001). Episodic Emergence in the Past 3000 Years at the Akkeshi Estuary, Hokkaido, Northern Japan. *Quaternary Research* **56,** 231-241.

Sawai, Y. (2002). Evidence for 17th-century tsunamis generated on the Kuril–Kamchatka subduction zone, Lake Tokotan, Hokkaido, Japan. *Journal of Asian Earth Sciences* **20,** 903-911.

Sawai, Y., Fujii, Y., Fujiwara, O., Kamataki, T., Komatsubara, J., Okamura, Y., Satake, K., and Shishikura, M. (2008). Marine incursions of the past 1500 years and evidence of tsunamis at Suijin-numa, a coastal lake facing the Japan Trench. *The Holocene* **18,** 517.

Scheffers, A., and Scheffers, S. (2006). Documentation of the impact of Hurricane Ivan on the coastline of Bonaire (Netherlands Antilles). *Journal of Coastal Research* **22,** 1437-1450.

Scileppi, E., and Donnelly, J. P. (2007). Sedimentary evidence of hurricane strikes in western Long Island, New York. *Geochemistry Geophysics Geosystems* **8**.

Shimoyama, S. (1994). Coastline and ground deformation after Jomon marine transgression in Northern Kyushu. *Quaternary Research* **33,** 351-360 (In Japanese).

Shimoyama, S., Iso, N., Noi, H., Takatsuka, K., Kobayashi, S., and Saeki, H. (1991). Marine quaternary system in the Fukuoka Torikai lowland and its post-

Pleistocene geomorphological formation, pp. 1-23. Kyushu University Faculty of Sciences Research Report

Shoku-Nihongi. (797). "Chronicle of Japan, continued, from 697-791 AD." The Transactions of the Asiatic Society of Japan.

Snyder, R. A., and Boss, C. L. (2002). Recovery and Stability in Barrier Island Plant Communities. *Journal of Coastal Research* **18,** 530-536.

Spiske, M., Borocz, Z., and Bahlburg, H. (2008). The role of porosity in discriminating between tsunami and hurricane emplacement of boulders - A case study from the Lesser Antilles, southern Caribbean. *Earth and Planetary Science Letters* **268,** 384-396.

Stahle, D. W., Cleaveland, M. K., Therrell, M. D., Gay, D. A., D'Arrigo, R. D., Krusic, P. J., Cook, E. R., Allan, R. J., Cole, J. E., and Dunbar, R. B. (1998). Experimental Dendroclimatic Reconstruction of the Southern Oscillation. *Bulletin of the American Meteorological Society* **79,** 2137-2152.

Stockdon, H. F., Sallenger, A. H., Holman, R. A., and Howd, P. A. (2007). A simple model for the spatially-variable coastal response to hurricanes. *Marine Geology* **238,** 1-20.

Stone, G. W., Liu, B., Pepper, D. A., and Wang, P. (2004). The importance of extratropical and tropical cyclones on the short-term evolution of barrier islands along the northern Gulf of Mexico, USA. *Marine Geology* **210,** 63-78.

Sugihara, K., Nakamori, T., Iryu, Y., Sasaki, K., and Blanchon, P. (2003). Holocene sea-level change and tectonic uplift deduced from raised reef terraces, Kikai-jima, Ryukyu Islands, Japan. *Sedimentary Geology* **159,** 5-25.

Suzuki, A., Yokoyama, Y., Kan, H., Minoshima, K., Matsuzaki, H., Hamanaka, N., and Kawahata, H. (2008). Identification of 1771 Meiwa Tsunami deposits using a combination of radiocarbon dating and oxygen isotope microprofiling of emerged massive Porites boulders. *Quaternary Geochronology* **3,** 226-234.

Taira, A. (2001). Tectonic evolution of the Japanese Island Arc system. *Annual Reviews of Earth and Planetary Sciences* **29,** 109-134.

Takishita, K., Tsuchiya, M., Kawato, M., Oguri, K., Kitazato, H., and Maruyama, T. (2007). Genetic Diversity of Microbial Eukaryotes in Anoxic Sediment of the Saline Meromictic Lake Namako-ike (Japan): On the Detection of Anaerobic or Anoxic-tolerant Lineages of Eukaryotes. *Protist* **158,** 51-64.

Thomson, J., Croudace, I. W., and Rothwell, R. G. (2006). A geochemical application of the ITRAX scanner to a sediment core containing eastern Mediterranean sapropel units. *SPECIAL PUBLICATION-GEOLOGICAL SOCIETY OF LONDON* **267,** 65.

Trenberth, K. E., Josey, S. A., P., A., Bojariu, R., Easterling, D. U., Tank, A. K., Parker, D. E., Rahimzadeh, F. I., Renwick, J. A., Rusticucci, M., Soden, B., and Zhai, P. (2007). Observations: surface and atmospheric climate change. *In* "Climate Change 2007: The Physical Science Basis: Contribution of Working Group I to the Fourth Assessment Report of the Intergovernmental Panel on Climate Change." (S. Solomon, Q. D., M. Manning, Z. Chen, M. Marquis, K. B. Averyt, M. Tignor, and H. L. Miller, Eds.), Cambridge, U.K.

Wang, B., and Chan, J. C. L. (2002). How Strong ENSO Events Affect Tropical Storm Activity over the Western North Pacific. *Journal of Climate* **15,** 1643-1658.

Watanabe, H. (1998). "Comprehensive List of Tsunamis to Hit the Japanese Islands." University of Tokyo Press, Tokyo (In Japanese).

Webster, J. M., Davies, P. J., and Konishi, K. (1998). Model of fringing reef development in response to progressive sea level fall over the last 7000 years-(Kikai-jima, Ryukyu Islands, Japan). *Coral Reefs* **17,** 289-308.

White, P. S. (1979). Pattern, process, and natural disturbance in vegetation. *The Botanical Review* **45,** 229-299.

Woodruff, J. D. (2008). "Tropical Cyclones within the Sedimentary Record: Analyzing Overwash Deposition from Event to Millennial Timescales." Ph.D. Thesis, Massachusetts Institute of Technology/Woods Hole Oceanographic Institution.

Woodruff, J. D., Donnelly, J. P., Emanuel, K., and Lane, P. (2008a). Assessing sedimentary records of paleohurricane activity using modeled hurricane climatology. *Geochemistry Geophysics Geosystems* **9**.

Woodruff, J. D., Donnelly, J. P., Mohrig, D., and Geyer, W. R. (2008b). Reconstructing relative flooding intensities responsible for hurricane-induced deposits from Laguna Playa Grande, Vieques, Puerto Rico. *Geology* **36,** 391-394.

Yokoyama, Y., Nakada, M., Maeda, Y., Nagaoka, S., Okuno, J., Matsumoto, E., Sato, H., and Matsushima, Y. (1996). Holocene sea-level change and hydro-isostasy along the west coast of Kyushu, Japan. *Palaeogeography, Palaeoclimatology, Palaeoecology* **123,** 4.

Yu, K. F., Zhao, J. X., Collerson, K. D., Shi, Q., Chen, T. G., Wang, P. X., and Liu, T. S. (2004). Storm cycles in the last millennium recorded in Yongshu Reef, southern

South China Sea. *Palaeogeography Palaeoclimatology Palaeoecology* **210,** 89-100.

Zhu, Y. Z., Nie, B. F., and Wang, Y. Q. (1991). Coral reef sediments respectively in the southern and northern parts of Nansha Islands. *In* "Symposium on Geology, Geophysics and Reef Islands of Nansha Islands and Adjacent Areas." pp. 224-232. Ocean Press, Beijing.

9. Figure and table captions

Fig. 1. (Left) Map of the western North Pacific showing study area (open red square). The locations of Nagasaki, Kagoshima Bay, and Tanegashima mentioned in text are identified by a, b, and c, respectively. (Left inset) Regional map of the Koshikijima Island archipelago. Lake Namakoike and Lake Kaiike (highlighted with open blue square) are located on the northern most island of Kamikoshiki. (Right) Bathymetric map of lakes Namakoike and Kaiike with chirp seismic tracklines and coring locations referenced in the text. Bathymetry obtained by Aramaki et al. (1969) and Oguri et al. (2002), and updated with seismic surveys from this study.

Fig. 2. (Black circles) Reconstructions of relative sea-level during the mid-Holocene for western Kyushu (Yokoyama, 1996), compared to (contours) glacial-isostatic model predictions for relative sea-level at 6000 yr BP (after Nakada, 1991, Ice models ARC3+ANT3B, Viscosity model A).

Fig. 3. Seismic surveys for Lake Namakoike and Lake Kaiike with interpretation below. Tracklines are shown in Figure 1. Green shading identifies top sedimentary unit described in text (Unit 1), and yellow shading identifies lower unit (Unit 2). Truncated stratigraphy and cut/fill features at the contact between the two units are suggestive of an erosional incision. Vertical lines indicate locations and approximate depths for cores NKI5 and KI2.

Fig. 4. NKI5 down-core profiles for Sr peak area integral (blue), percent coarse sediment (red), and x-ray grayscale density (green). Note Sr concentrations increase to the left, and percent coarse sediment and x-ray density to the right. X-ray grayscale density is relative. Profiles for NKI5 are superimposed on seismic survey from Basin-NB (Fig. 1 and 3), with core position in the middle of the y-axes between Sr and percent coarse profiles. Dashed white line denotes depth of erosional contact in NKI5 at the base of Unit 1 (Fig. 3).

Fig. 5. Higher-resolution analyses of the upper 50 cm of NKI5. (From left to right) Depth profiles of percent coarse sediment, x-ray gray-scale relative density, Sr, , and detectable ^{137}Cs activity (error bars in gray). Age model on right is based on accumulation rate of 2.3 mm yr-1 determined from the position of the 1963 AD ^{137}Cs peak (dashed line).

Fig. 6. Age versus depth plot of chronological data for cores NKI5 (black) and KI2 (gray). Horizonal solid lines denote 1 standard deviation for radiocarbon ages. Numbers in plot coincide with sample identification in Table 1. The 1963 AD peak in 137Cs is noted with a square. Depth for the erosional contact at the base of Unit 1 (Fig. 3) at NKI5 and KI2 are noted with dashed black and gray lines, respectively.

Fig. 7. Sr peak integrated area for cores NKI5 (black) and KI2 (gray) (See Fig.1 for locations). Thicker vertical black and gray lines to the right and left of the figure indicate intervals with fine-scale (<1 mm) laminations for core NKI5 and KI2, respectively. Solid arrows represent the depth of radiocarbon-dated samples from each core. Thin dashed lines indicate depths of equal age between cores based on the age model presented in Fig. 6.

Fig. 8. a) Sr time-series for cores NKI5 (black) and KI2 (gray), compared to b) El Niño reconstructions from Laguna Pallcocha, Ecuador (Moy et al., 2002), and c) proxy records of hurricane-induced sedimentation from Laguna Playa Grande, Vieques, Puerto Rico (Donnelly and Woodruff, 2007). Solid arrows in each plot identify age controls. The El Niño proxy is based upon red clastic sediments deposited during El Niño events. Shaded line in plot is red color intensity, and solid line is the 50 point running average. Peaks in Laguna Playa Grande bulk grain-size above roughly the sand/silt transition (>70 μm) represent hurricane-induced deposits (Woodruff et al., 2008). Vertical shaded bars in plots represent periods of increased El Niño frequency following 4000 yr BP, which are generally

concurrent with both an increase in typhoon-induced deposition at the Kamikoshiki site, and a decrease in hurricane-induced deposition in the western North Atlantic.

Fig. 9. a) Guangdong typhoon landfalls (twenty-one year running average) after Liu et al. (2001), and b) Sr peak integrated area for cores NKI5 (black) and KI2 (gray). Solid arrows at bottom of plot denote age controls.

Table 1. Kamikoshiki radiocarbon dates and calibrated ages (1 sigma range) in calendar years Before Present (yr BP) using IntCal04 (Reimer et al., 2004), where 1950 AD is defined as "Present" by convention.

Figure 1

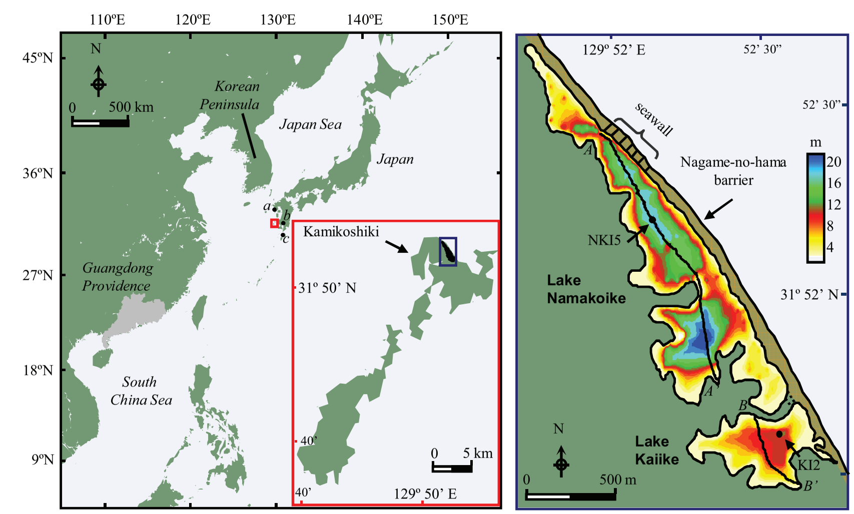

110ºE
120ºE
130ºE
140ºE
150ºE
45ºN
36ºN
27ºN
18ºN
9ºN
N
0
500 km
Korean
Peninsula
Japan Sea
Japan
a
b
c
Guangdong
Providence
South
China Sea
Kamikoshiki
31º 50' N
40'
0
5 km
40'
129º 50' E
129º 52' E
52' 30"
seawall
Nagame-no-hama
barrier
m
20
16
12
8
4
NK15
Lake
Namakoike
31º 52' N
A
A'
B
B'
Lake
Kaiike
KI2
N
0
500 m

Figure 2

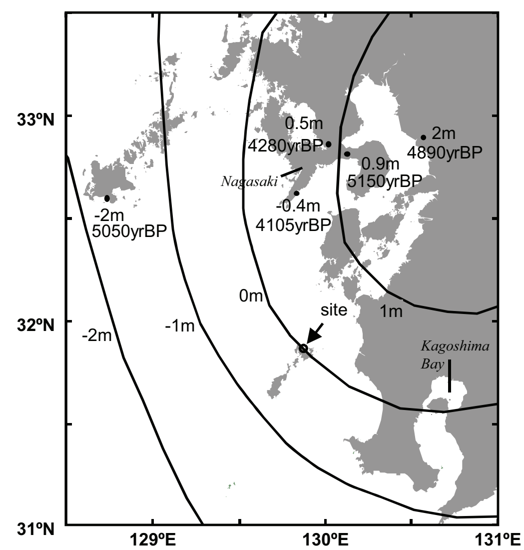

Figure 2: Woodruff, Donnelly and Okusu, (2008)

Figure 3

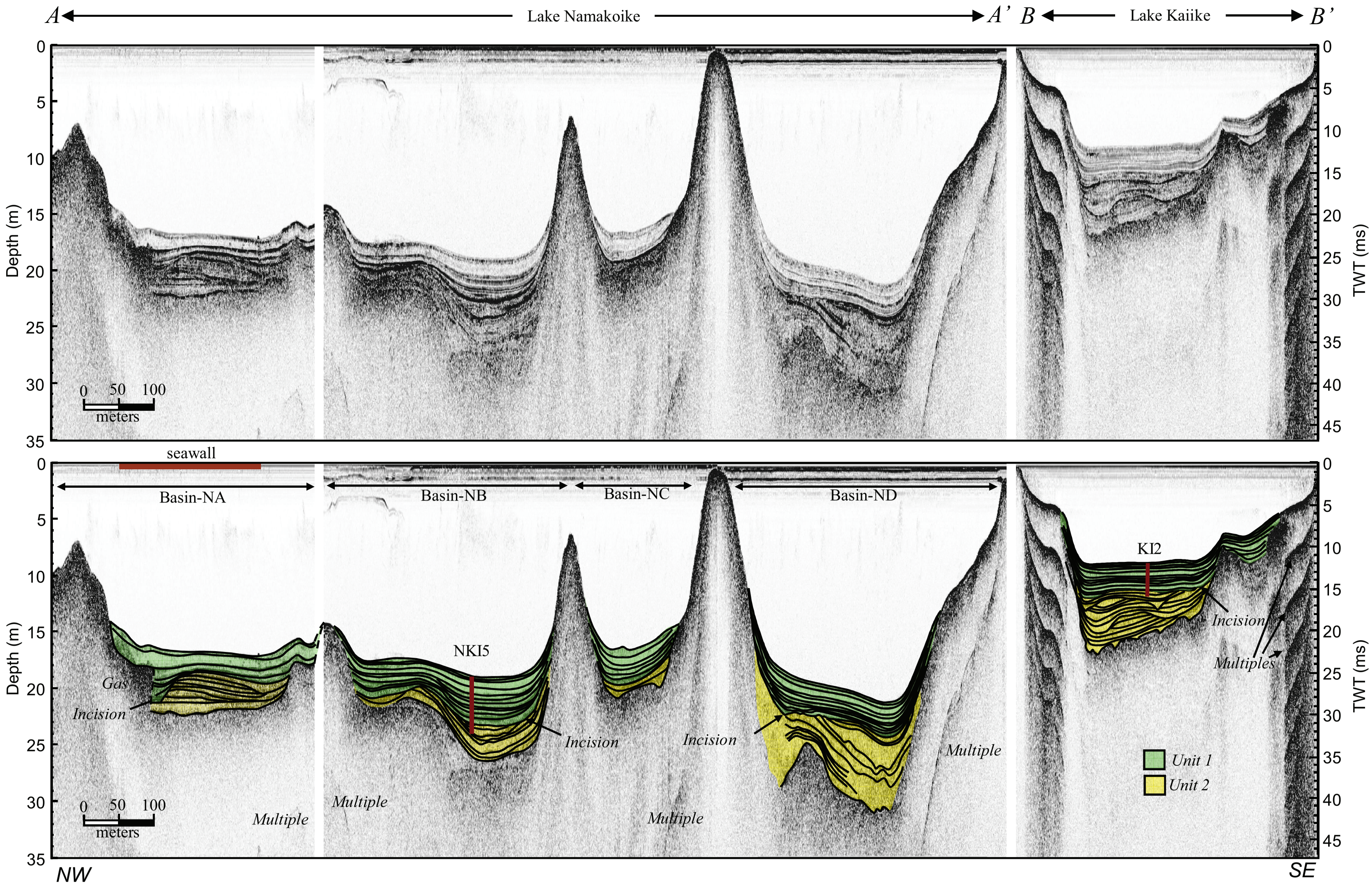

Figure 3: Woodruff, Donnelly and Okusu, (2008)

Figure 4

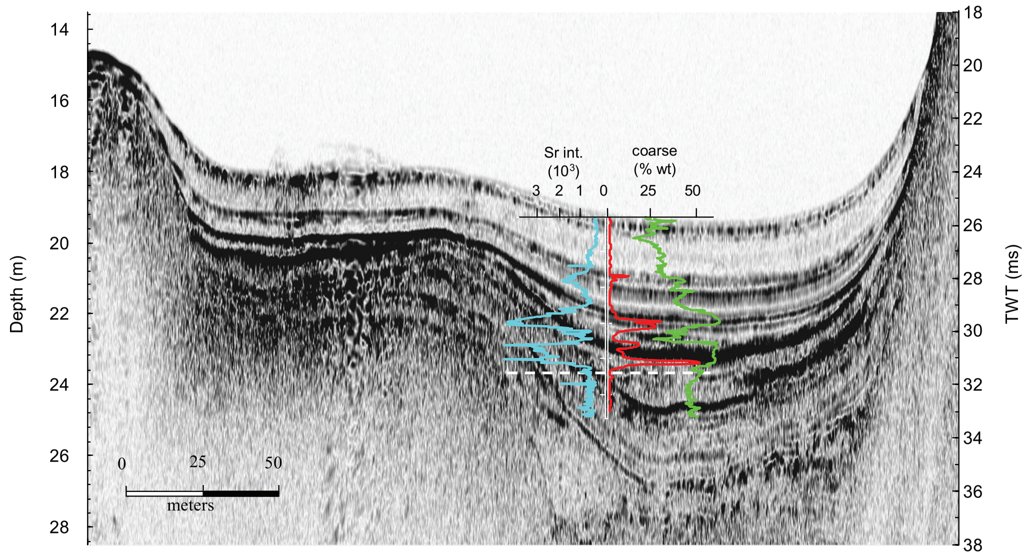

Figure 4: Woodruff, Donnelly and Okusu, (2008)

Figure 5

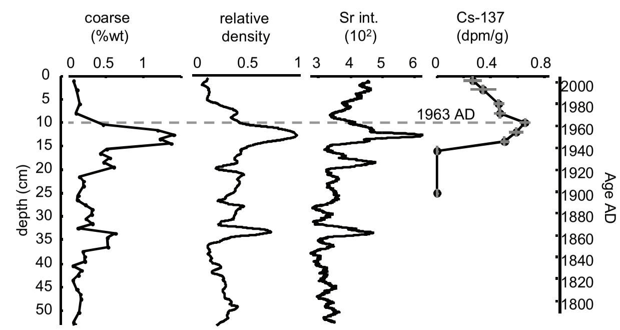

Figure 5: Woodruff, Donnelly and Okusu, (2008)

Figure 6

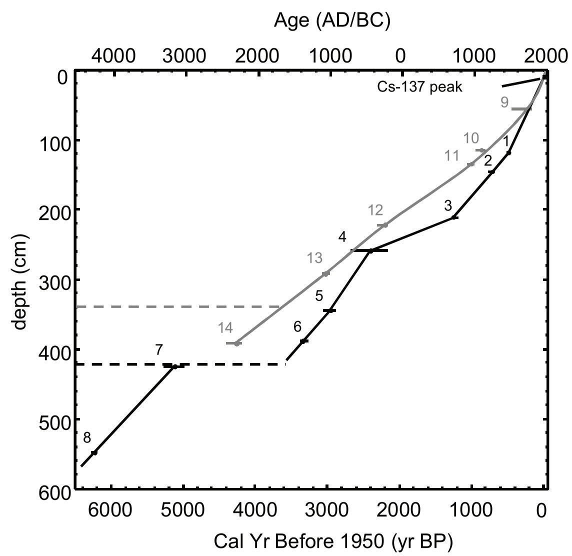

Figure 6: Woodruff, Donnelly and Okusu, (2008)

Figure 7

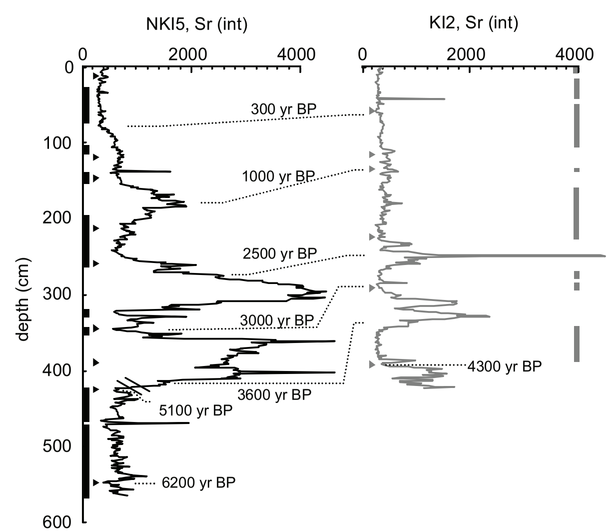

Figure 7: Woodruff, Donnelly and Okusu, (2008)

Figure 8

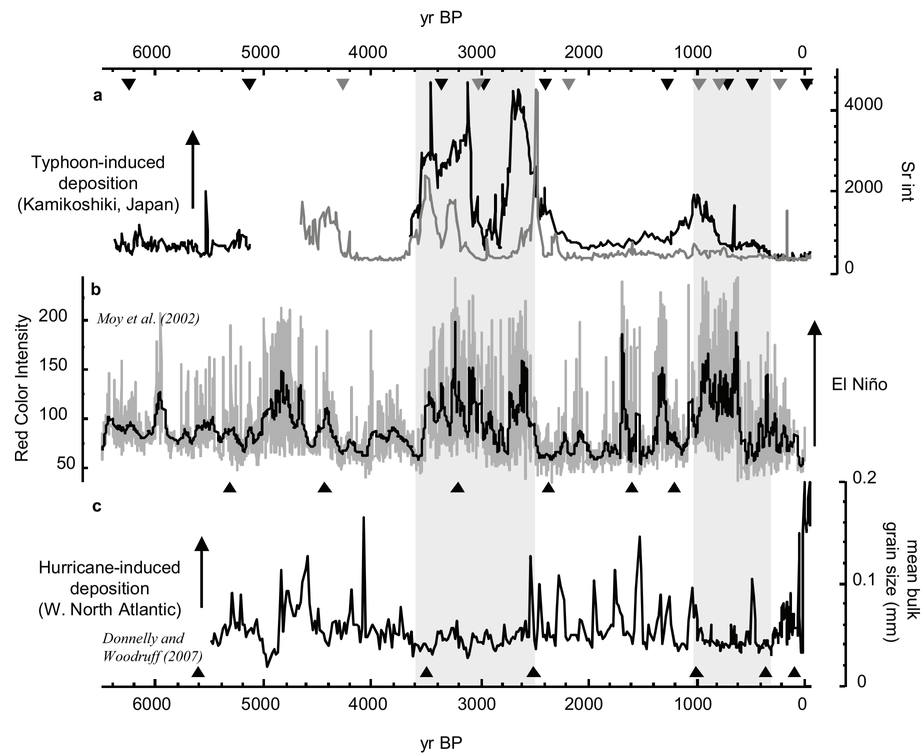

Figure 8: Woodruff, Donnelly and Okusu, (2008)

Figure 9

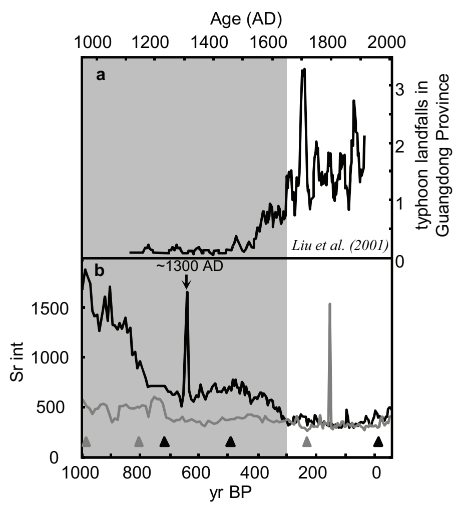

Figure 9: Woodruff, Donnelly and Okusu (2008)

Table 1

KAMIKOSHIKI RADIOCARBON RESULTS

Index Number	Lab Number	Core	Depth (cm)	14C age	Cal yr BP (1σ)	δ13C (‰)	Material Dated
1	OS-62015	NKI5	118-119	410±25	(473-507)	-26.64	leaf
2	OS-57839	NKI5	146-147	820±30	(690-756)	-28.7	leaf
3	OS-62101	NKI5	211-213	1290±30	(1182-1277)	-28.52	leaf
4	OS- 57952	NKI5	258-259	2330±100	(2158-2675)	-26.27	woody debris
5	OS- 57888	NKI5	344-345	2850±40	(2881-3058)	-25.88	woody debris
6	OS-67805	NKI5	388-389	3100±35	(3266-3371)	-28.74	leaf
7	OS- 62016	NKI5	423-425	4450±30	(4974-5267)	-27.79	woody debris
8	OS- 57912	NKI5	547-548	5390±30	(6185-6274)	-26.86	woody debris
9	OS- 61946	KI2	56-57	270±35	(157-426)	-30.67	leaf
10	OS- 57911	KI2	115-116	980±30	(802-932)	-26.78	woody debris
11	OS- 62217	KI2	134-135	1090±30	(961-1052)	-28.92	leaf
12	OS-62111	KI2	223-224	2210±25	(2156-2307)	-29.96	bark
13	OS- 57782	KI2	291-292	2890±30	(2969-3067)	-29.06	twig
14	OS- 57889	KI2	392-392	3860±30	(4193-4405)	-28.31	woody debris